PHYSICAL REVIEW C VOLUME 50, NUMBER 3 SEPTEMBER 1994

Coulomb breakup mechanism of neutron drip-line nuclei

T. Kido
Graduate School of Science and Technology, Niigata University, Niigata 950-21, Japan

K. Yabana and Y. Suzuki
Department of Physics, Niigata University, Niigata 950-21, Japan
(Received 10 May 1994)

The mechanism of the Coulomb breakup reaction of the projectile nuclei with neutron halo structure is investigated by the time-dependent Schrödinger equation in three-dimensional space. The time evolution of the internal wave function between the core nucleus and the halo neutron is calculated in the target Coulomb field treated as the time-dependent external field. Calculations are done for the ^{11}Be+^{208}Pb system for which an experiment has been done recently. The calculated results support the picture of free-particle breakup mechanism: Only the core nucleus is affected by the target Coulomb field, while the halo neutron moves independently. As a result, we obtain large transverse and small longitudinal difference in the relative velocity between the core and the neutron after the breakup. The origin of the longitudinal velocity difference observed experimentally is left unresolved in our approach.

PACS number(s): 25.60.+v, 25.70.De

In the light nuclei around the neutron drip line, the neutron halo structure has been observed systematically [1]. Besides the spatially extended density distribution of the halo neutron, the drip-line nuclei have such characteristics that they easily breakup into the core nucleus and the halo neutron(s). Especially the large breakup cross section has been observed in the Coulomb excitation [2]. The Coulomb breakup is induced mainly by the electric dipole component of the target Coulomb field. The large Coulomb breakup cross section is related to the $E1$ strength distribution at low excitation energy [3]. A question concerning the property of this low lying dipole strength is whether or not it has a resonance character representing the vibration of the halo neutron and the core [4].

In the recent coincident measurements of the core and the halo neutron, the significant difference in the longitudinal velocity distribution between them has been observed in the Coulomb breakup reaction of ^{11}Li [5] and ^{11}Be [6]. It has been explained in terms of the Coulomb postacceleration effect by assuming the direct breakup mechanism [5,6]. Before the closest approach point where the breakup is assumed to occur, the projectile is decelerated by the target Coulomb field. After the closest approach point the core and the halo neutron move independently. Since only the core nucleus is accelerated by the target Coulomb field, the velocity difference is expected to occur between the core and the neutron. On the other hand, if the breakup proceeds by way of the resonant state, the core and the halo neutron would move together until they decay and the velocity difference would be small. Therefore, the measurements of the velocity difference are expected to be useful as a clock to measure the lifetime of the resonant state.

The Coulomb postacceleration is a higher order effect in the perturbative treatment of the Coulomb excitation. To calculate the higher order terms is not easy in the breakup reaction into continuum states. Several approaches have been applied including a classical treatment of the breakup [7], a distorted wave Born approach [8], and also a simplified treatment of higher order perturbations [9]. Recently, Bertsch and Bertulani [10] have analyzed the issue by solving the time-dependent Schrödinger equation with the grid for both spatial and time variables. Their analysis was restricted to one spatial dimension. In this paper we report our analysis for the Coulomb breakup reaction in the time-dependent Schrödinger equation with full three spatial dimensions. An analysis of three spatial dimensions has also been reported recently in Ref. [11] where a simplified internal Hamiltonian is assumed between the core and the neutron.

Bertsch and Bertulani [10] have found that the velocity difference is even larger than expected by the direct breakup mechanism, and explained the result by the "free particle" breakup mechanism in contrast to the direct or resonant mechanism. To understand this mechanism, let us imagine the weakly bound limit of the halo neutron. The neutron keeps its velocity throughout the reaction; only the core is acted by the target Coulomb field. The core receives the momentum transfer only for the transverse direction at high energy. Consequently, we expect a large velocity difference in the transverse direction and a small difference in the longitudinal direction.

We summarize in Table I the classical estimates of the relative momentum between the core and the neutron after

TABLE I. The classical estimates for the longitudinal and transverse relative momentum between the neutron and the core nucleus after the breakup due to various reaction mechanisms. The momentum k_C is defined by $k_C=[m_n/(m_n+M_C)]Z_TZ_Ce^2/\hbar bv$, where Z_C (Z_T) is the core (target) charge number, m_n and M_C are the mass of the neutron and the core, respectively, v is the incident velocity of the projectile, and b is the impact parameter. The zero momentum for the resonant breakup is the limiting case of long lifetime.

	Resonant	Direct	Free particle
$\Delta k_\parallel$	0	k_C	0
$\Delta k_\perp$	0	k_C	$2k_C$

the breakup in the various pictures for the breakup. In the case of the resonant breakup the velocity difference depends on the lifetime. The long lifetime limit is assumed in the table. Note that the longitudinal velocity difference exists only in case of the direct breakup.

We analyze the Coulomb breakup reaction of ^{11}Be+^{208}Pb at 72 MeV/nucleon done at RIKEN [6]. The ^{11}Be nucleus is understood as a weakly bound system of ^{10}Be core and the single halo neutron. The relative motion between them is described with

$$i\hbar \frac{\partial}{\partial t} \psi(\mathbf{r},t) = \{h(\mathbf{r}) + V_{\mathrm{ext}}(\mathbf{r},t)\}\psi(\mathbf{r},t), \tag{1}$$

where $\mathbf{r}$ is the radius vector of the neutron measured from ^{10}Be and $h(\mathbf{r})$ the internal Hamiltonian describing the relative motion. We assume the straight line trajectory of the impact parameter $\mathbf{b}$ for the motion between the center of masses of ^{11}Be and ^{208}Pb. V_{ext} represents the target Coulomb field moving in the velocity $\mathbf{v}$,

$$V_{\mathrm{ext}}(\mathbf{r},t) = \frac{Z_C Z_T e^2}{|(m_n/M_C)\mathbf{r} - \mathbf{b} - \mathbf{v}t|} - \frac{Z_C Z_T e^2}{|\mathbf{b}+\mathbf{v}t|}, \tag{2}$$

where Z_T and Z_C are the charge numbers of the target and the core, and m_n and M_C are the masses of the neutron and the core, respectively. We expand Eq. (2) in multipoles and take the dipole and quadrupole fields into account.

The potential energy in h, assumed to be of spherical Woods-Saxon shape, is chosen to reproduce the basic property of ^{11}Be. The ground state of ^{11}Be is famous for its anomalous positive parity. The negative parity excited state exists close to the ground state. To reproduce such features with the spherical potential, the depth of the Woods-Saxon potential is chosen as l dependent. The potential of $l=0$ is determined to locate $1s$ orbital at the ground state energy, 0.503 MeV below the $n+{}^{10}$Be threshold. The potential of $l=1$ is chosen to locate the $0p$ orbital at the energy of the first excited $1/2^-$ state of ^{11}Be lying at 0.183 MeV below the $n+{}^{10}$Be threshold. The potential of $l>1$ is set the same as that of $l=1$. The radius and diffuseness parameters are fixed to $r_0=1.2$ fm and $a=0.6$ fm. No ls potential is included.

The time development of the wave function in a short interval is approximated as

$$\begin{aligned} \psi(\mathbf{r},t+\Delta t) &= \exp\left[-\frac{i}{\hbar}\{h(\mathbf{r})+V_{\mathrm{ext}}(\mathbf{r},t)\}\Delta t\right]\psi(\mathbf{r},t) \\ &\simeq \exp\left[-\frac{i}{\hbar}h(\mathbf{r})\Delta t\right] \\ &\quad \times \exp\left[-\frac{i}{\hbar}V_{\mathrm{ext}}(\mathbf{r},t)\Delta t\right]\psi(\mathbf{r},t). \end{aligned} \tag{3}$$

The successive operation implied in Eq. (3) is performed with use of a partial wave expansion for the wave function,

$$\psi(\mathbf{r},t) = \sum_{lm} \frac{u_{lm}(r,t)}{r} Y_{lm}(\hat{r}). \tag{4}$$

The maximum partial wave to be included is determined by checking the convergence of calculation. The inclusion of the waves up to $l_{\max}=4$ is sufficient for our problem. The radial wave function, $u_{lm}(r,t)$, is discretized in radial variable. The time evolution by the external field, $\exp[-iV_{\mathrm{ext}}\Delta t/\hbar]$, is evaluated by expanding the exponential function up to linear order in Δt. The evolution by the internal Hamiltonian is diagonal in the angular momentum space and each radial wave function evolves independently. We use the following formula [12]:

$$u_{lm}(r,t+\Delta t) \simeq \frac{1+h_l\Delta t/2i\hbar}{1-h_l\Delta t/2i\hbar} u_{lm}(r,t), \tag{5}$$

where h_l is the radial part of the internal Hamiltonian with angular momentum l.

We took the radial mesh of 0.4 fm and the maximum radius $r_{\max}=800$ fm. The time mesh is $\Delta t/\hbar = 0.01$ MeV^{-1} and the time range is -10 MeV$^{-1}<T/\hbar<10$ MeV^{-1}. The projectile velocity is about $v/c\sim 0.37$. At the initial and final stage of the calculation the target nucleus is apart from the projectile center of mass by about 750 fm in the longitudinal direction.

Starting with the ground state wave function $\psi(\mathbf{r},-\infty)=\phi_0(\mathbf{r})$, we calculate the time development of the wave function $\psi(\mathbf{r},t)$ for a target trajectory specified by the impact parameter $\mathbf{b}$. We express it as $|\psi(\mathbf{b},t)\rangle$. The breakup wave function is constructed by eliminating the bound state components

$$|\psi_{\mathrm{BU}}(\mathbf{b},t)\rangle = \left(1 - \sum_{i\in \mathrm{bound}} |\phi_i\rangle\langle\phi_i|\right)|\psi(\mathbf{b},t)\rangle. \tag{6}$$

We define the momentum distribution by

$$\frac{dP(\mathbf{k},t)}{d\mathbf{k}} = |\langle \mathbf{k}|\psi_{\mathrm{BU}}(\mathbf{b},t)\rangle|^2 \tag{7}$$

with the plane wave state $|\mathbf{k}\rangle$. A long time after the collision the breakup wave function becomes time independent except for a phase factor. The corresponding momentum distribution of Eq. (7) also becomes time independent and is denoted as $dP(\mathbf{b},\mathbf{k})/d\mathbf{k}$. The integration of Eq. (7) over $\mathbf{k}$ yields the total breakup probability at the impact parameter $\mathbf{b}$, and is equal to the norm of the breakup wave function, $\langle\psi_{\mathrm{BU}}|\psi_{\mathrm{BU}}\rangle$. Integrating it over the impact parameter yields the total breakup cross section.

We first show the calculation of the momentum distribution for $b=12$ fm, where the nuclear breakup probability is expected to become small. The corresponding classical shift of the relative momentum k_C is 0.046 fm^{-1}. We choose the reaction plane as the x-z plane, $\mathbf{b}$ in x direction and the target velocity in the negative z direction, $\mathbf{v}=(0,0,-v)$.

Figure 1 shows the longitudinal momentum distribution

$$P(k_z) = \int dk_x dk_y \frac{dP(\mathbf{k},t)}{d\mathbf{k}},$$

at the closest approach time (dashed curve) and the final time of the calculation (solid curve). The integral of $P(k_z)$ over k_z gives the breakup probability, 0.063 in this case. The lon-

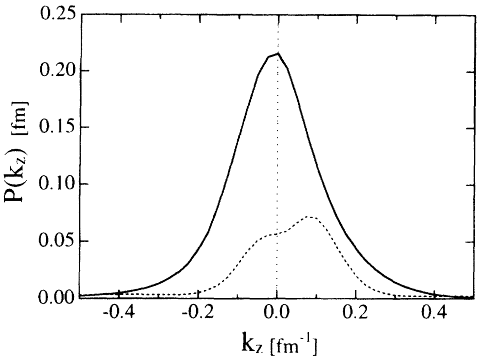

FIG. 1. The longitudinal momentum distribution of the relative motion between the neutron and core nucleus. The dashed curve is the one at the closest approach of the target nucleus, and the solid curve at the final stage of the calculation.

gitudinal momentum distribution is nearly symmetric after the collision. The peak lies at almost zero momentum. The slight shift to the negative direction is seen, which is considered to reflect the postacceleration effect. However, the shift is by far smaller than $\Delta k_{\parallel}=0.046$ fm^{-1} expected from the direct breakup picture. At the closest approach the breakup probability becomes already substantial and the appreciable shift of the distribution to the positive direction is observed. These features can be understood by the free-particle breakup picture. The assumption that the neutron is decelerated together with the core nucleus before the closest approach point, which is needed for the postacceleration mechanism in the direct breakup picture, is thus largely broken in the present case.

Figure 2 shows the transverse momentum distribution in the reaction plane,

$$P(k_x)=\int dk_y dk_z \frac{dP(\mathbf{k},t)}{d\mathbf{k}} .$$

The distribution consists of two peaks and the large asymmetry is seen. The two peaks in the momentum distribution can be understood by the p wave character of the breakup wave function because the main component of the breakup wave function would be proportional to $x\phi_0(r)$ by the dipole excitation. The shape of the momentum distribution at the closest approach point, shown by dashed curve, is quite close to that of the longitudinal direction. This is again consistent with the free-particle breakup picture. The average shift of the momentum,

$$\langle k_x\rangle=\int d\mathbf{k}k_x\frac{dP}{d\mathbf{k}} \Big/ \int d\mathbf{k}\frac{dP}{d\mathbf{k}} ,$$

is calculated to be 0.051 fm^{-1}, lying between k_C and $2k_C$, the direct and the free-particle breakup pictures.

The reaction of the free-particle breakup looks rather simple when it is viewed in the laboratory frame (target rest frame). The halo neutron proceeds along the almost straight line. The core moves along the Coulomb trajectory determined by the core and the target nucleus. We thus expect that the neutron angular distribution is more forward peaked than that of the core.

Our results are consistent with the existing calculations. The large transverse momentum is reported in Ref. [10] and the small longitudinal momentum is obtained in Refs. [8,11]. In contrast to Ref. [11] where the attractive interaction between the halo neutron and the core is not included except for s wave, we included the attractive interaction for all partial waves but the conclusion of the small shift in the longitudinal momentum did not change.

Our calculation includes both the dipole and quadrupole components of the target Coulomb field. We repeated calculations by switching off the quadrupole field and found that the effect of the quadrupole field is very small. We cannot explain the longitudinal velocity difference between the core and the neutron, which has been observed experimentally [5,6]. The calculation does not support the explanation that the velocity difference arises from the postacceleration in the direct breakup picture mechanism.

We next show the breakup cross section as a function of the relative energy of the fragments

$$\frac{d\sigma_{\mathrm{BU}}}{dE}=\int_{b_{\mathrm{min}}}^{\infty} 2\pi b db \int d\mathbf{k}\delta\left(\frac{\hbar^2k^2}{2\mu}-E\right)\frac{dP(\mathbf{b},\mathbf{k})}{d\mathbf{k}} . \quad (8)$$

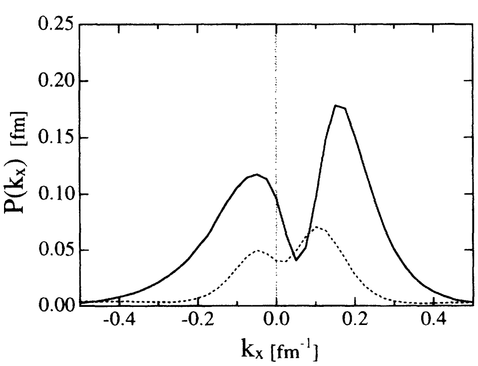

FIG. 2. The transverse momentum distribution of the relative motion between the neutron and core nucleus. The dashed curve is the one at the closest approach of the target nucleus, and the solid curve at the final stage of the calculation.

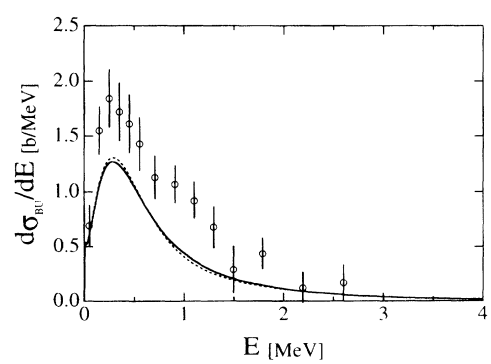

FIG. 3. The Coulomb breakup cross section as a function of the relative motion energy between the neutron and core nucleus. The solid curve is the result of the time-dependent Schrödinger calculation and the dashed curve the result of the perturbation calculation. The measured cross sections are from Ref. [6].

We took $b_{\text{min}}=12$ fm. To calculate the cross section, the breakup probabilities for wide impact parameter region are needed, because of the long range character of the Coulomb interaction. However, the calculation at large impact parameter involves difficulty in the present approach solving the time dependent Schrödinger equation numerically. The Coulomb interaction, though weak, acts for a long period at large impact parameter, so that the calculation of a very long period is required to obtain convergent results. Fortunately, we can use the perturbation theory at large b where the Coulomb interaction is weak enough. In the practical calculation, we calculate $dP(\mathbf{b},\mathbf{k})/d\mathbf{k}$ by the time-dependent Schrödinger equation for $b<30$ fm, and by the perturbation theory for $b>30$ fm. We confirmed that both calculations give the results quite close to each other at $b=30$ fm.

The calculated result is compared with the measured cross section in Fig. 3. The calculation reproduces a strong peak at low excitation energy in agreement with the measurement [6], though the magnitude of the calculated cross section is somewhat smaller than the measured value. For the sake of comparison we also show the result of the usual perturbation treatment taking only the dipole excitation into account. The energy dependence of the cross section is quite similar between the time-dependent Schrödinger approach and the perturbation calculation, though the transverse momentum distribution shows large asymmetry at the small impact parameter which indicates the importance of nonperturbative effect.

In summary, we calculated the Coulomb breakup of the neutron halo nucleus, ^{11}Be, by solving the time-dependent Schrödinger equation in three spatial dimensions. The target Coulomb field was treated as the time-dependent external field. The momentum distribution between the neutron and the core nucleus is calculated. The large transverse and small longitudinal shifts of the average momentum are found. The result is understood naturally in the free-particle breakup picture which assumes very weak interaction between the neutron and the core. The neutron does not receive forces from the target nucleus and proceeds along the nearly straight line trajectory, while the core proceeds along the Coulomb trajectory between the core and the target nucleus. We could not explain the origin of the experimentally observed longitudinal velocity difference between the neutron and the core. Our calculation does not support the postacceleration in the direct breakup picture which has been employed to explain the velocity difference.

[1] P. G. Hansen, Nucl. Phys. **A553**, 89c (1993).
[2] T. Kobayashi *et al.*, Phys. Lett. B **232**, 51 (1989).
[3] Y. Suzuki and Y. Tosaka, Nucl. Phys. **A517**, 599 (1990); G. F. Bertsch and J. Foxwell, Phys. Rev. C **41**, 1300 (1990).
[4] K. Ikeda, Nucl. Phys. **A538**, 355c (1992); P. G. Hansen and B. Jonson, Europhys. Lett. **4**, 409 (1987).
[5] K. Ieki *et al.*, Phys. Rev. Lett. **70**, 730 (1993); D. Sackett *et al.*, Phys. Rev. C **48**, 118 (1993).
[6] T. Nakamura *et al.*, Phys. Lett. B **331**, 296 (1994).
[7] G. Baur, C. A. Bertulani, and D. M. Kalassa, Nucl. Phys. **A550**, 527 (1992).
[8] R. Shyam, P. Banerjee, and G. Baur, Nucl. Phys. **A540**, 341 (1992).
[9] S. Typel and G. Baur, Nucl. Phys. **A573**, 486 (1994).
[10] G. F. Bertsch and C. A. Bertulani, Nucl. Phys. **A556**, 136 (1993).
[11] L. F. Canto, R. Donangelo, A. Romanelli, and H. Schulz, Phys. Lett. B **318**, 415 (1993).
[12] S. E. Koonin, *Computational Physics* (Benjamin/Cummings, New York, 1986).